the FEBS Journal

Type III secretion system translocator has a molten globule conformation both in its free and chaperone-bound forms

Eric Faudry[1]*, Viviana Job[2]*, Andréa Dessen[2], Ina Attree[1] and Vincent Forge[3]

1 CEA Grenoble, DSV-iRTSV, Laboratoire de Biochimie et Biophysique des Systèmes Intégrés, UMR5092 (CNRS, CEA, Université Joseph Fourier), Grenoble, France
2 Institut de Biologie Structurale Jean-Pierre Ebel, UMR5075 (CNRS, CEA, Université Joseph Fourier), Grenoble, France
3 CEA Grenoble, DSV-iRTSV, Laboratoire de Chimie et Biologie des Métaux, UMR5249 (CNRS, CEA, Université Joseph Fourier), Grenoble, France

Keywords
chaperones; molten globule; pore-forming toxins; translocator; type III secretion system

Correspondence
V. Forge, CEA Grenoble, DSV-iRTSV, Laboratoire de Chimie et Biologie des Métaux (UMR 5249), 17 rue des martyrs, 38054 Grenoble Cedex 9, France
Fax: +33 4 38 78 54 87
Tel: +33 4 38 78 94 05
E-mail: vincent.forge@cea.fr

*These authors contributed equally to this work

(Received 22 March 2007, revised 11 May 2007, accepted 17 May 2007)

doi:10.1111/j.1742-4658.2007.05893.x

Type III secretion systems of Gram-negative pathogenic bacteria allow the injection of effector proteins into the cytosol of host eukaryotic cells. Crossing of the eukaryotic plasma membrane is facilitated by a translocon, an oligomeric structure made up of two bacterial proteins inserted into the host membrane during infection. In *Pseudomonas aeruginosa*, a major human opportunistic pathogen, these proteins are PopB and PopD. Their interactions with their common chaperone PcrH in the cytosol of the bacteria are essential for the proper function of the injection system. The interaction region between PopD and PcrH was identified using limited proteolysis, revealing that the putative PopD transmembrane fragment is buried within the PopD/PcrH complex. In addition, structural features of PopD and PcrH, either individually or within the binary complex, were characterized using spectroscopic methods and 1D NMR. Whereas PcrH possesses the characteristics of a folded protein, PopD is in a molten globule state either alone or in the PopD/PcrH complex. The molten globule state is known to enable the membrane insertion of translocation/pore-forming domains of bacterial toxins. Therefore, within the bacterial cytoplasm, PopD is preserved in a state that is favorable to secretion and insertion into cell membranes.

Type III secretion systems (TTSS) are carried by Gram-negative pathogenic bacteria responsible for life-threatening diseases (*Salmonella* spp., *Shigella* spp., *Yersinia* spp., *Pseudomonas aeruginosa*) [1]. These 'molecular syringes', also called injectisomes, have been linked to the injection of toxic effector proteins into the host cell. Effectors are thought to be secreted through a needle-like hollow conduit, and crossing of the target plasma membrane is facilitated by a proteinaceous structure believed to form a pore [2,3]. This structure, called translocon, is formed by two bacterial proteins inserted into the host membrane during infection. In *P. aeruginosa*, a major human opportunistic pathogen, the translocator proteins are PopB and PopD, which carry two and one putative transmembrane helices, respectively [4]. Each of the proteins is able to form ring-like structures on the surface of liposomes [5] and associate to form, in synergy, pores of defined size in lipid vesicles [6]. *In vivo*, it is believed that these proteins can be found in three different states: (a) associated in 1 : 1 complexes with their common chaperone PcrH in the bacterial cytoplasm; (b) dissociated from PcrH during secretion through the TTSS needle; and (c) inserted as a translocation pore within the host cell plasma membrane [5].

Abbreviations
ANS, 8-anilinonaphthalene-1-sulfonate; CBD, chaperone-binding domain; GST, glutathione *S*-transferase; TPR, tetratricopeptide repeats; TTSS, type III secretion system.

Type III secretion chaperones are necessary for the assembly and functioning of the injectisome. Three different chaperone classes can be distinguished, depending on the nature of their substrates: effectors, translocators or needle protein subunits [1]. Class I chaperones bind to effectors and such complexes have been extensively characterized.

Class II chaperones, for which no structures are available, bind to the translocators and are predicted to mostly fold into three tandem tetratricopeptide repeats (TPRs) [7]. Binding of the translocators to their chaperones blocks the membrane recognition capabilities of the former, increases their stability within the bacterial cytosol and prevents their premature association within the bacterial cytosol, i.e. before they reach the host cell plasma membrane [5,8–10].

In this study, structural features of PopD were investigated by taking advantage of the availability of the purified PopD/PcrH equimolar complex as well as of the individual proteins [5]. PopD–PcrH interaction regions were identified by limited proteolysis and the results indicate that the PopD transmembrane segment is buried within PcrH. Whereas PcrH possesses the features of a folded protein, PopD folds into a molten globule in the presence or absence of PcrH. Thus, within the bacterial cytoplasm, PopD is maintained in a monomeric state through association with PcrH, which prevents its premature oligomerization while keeping it in a state that is favorable to its secretion and subsequent insertion into the host cell membrane.

Results

Characterization of the PopD/PcrH interface

The region of PopD that interacts with PcrH in the 1 : 1 complex was identified by limited proteolysis combined with MS analysis and N-terminal sequencing. Digestion of the PopD/PcrH complex with trypsin was monitored by SDS/PAGE analysis of samples taken at different times (Fig. 1A). PcrH exhibited high resistance to proteolysis. After 3 h of treatment with trypsin, the predominant species were PcrH lacking the N-terminal His-tag ($PcrH_{1-167}$) and a form that also lacked the last seven residues ($PcrH_{1-160}$) (Fig. 1). In contrast to PcrH, PopD was rapidly degraded (Fig. 1A). In order to identify the regions of PopD that were protected from proteolysis due to interaction with PcrH, the last sample obtained after 3 h of digestion was subjected to gel-filtration chromatography. The protein peak corresponding to the high molecular mass species was analyzed by SDS/PAGE and the polypeptides were identified by MS and N-terminal sequencing (Fig. 1B).

The localization of the potential trypsin-cleavage sites within the sequence of PopD and PcrH are shown in Fig. 2A. Upon treatment of the PopD/PcrH complex with trypsin and gel-filtration chromatography, three small fragments of PopD were detected: $PopD_{28-147}$, $PopD_{28-107}$ and $PopD_{28-95}$ (Fig. 1B). Interestingly, within the N-terminal region of PopD, only one site was accessible to protease (at residue 28), whereas many sites were accessible in the C-terminal portion, from position 147 to 295. Notably, chaperone-free PopD is entirely degraded upon the action of the trypsin (data not shown). As described above, PcrH exhibited a much higher resistance to protease. Among potential cleavage sites (Fig. 2B), trypsin treatment removed the N-terminal His-tag of PcrH and subsequently the last seven residues (Fig. 1B). Longer incubation times (data not shown) led to removal of part of the first predicted α helix (generating $PcrH_{21-160}$) and subsequent removal of part of the last predicted helix (generating fragment $PcrH_{21-131}$). These

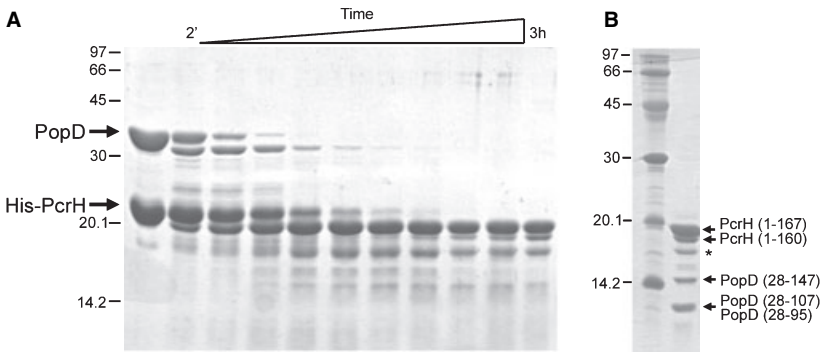

Fig. 1. Limited proteolysis of PopD/PcrH. (A) The PopD/PcrH complex was incubated with trypsin for up to 3 h and analyzed by SDS/PAGE. (B) After 3 h, complexes were purified by gel filtration and the protein bands were identified by MS and N-terminal sequencing. The band indicated by an asterisk corresponds to a PcrH fragment as shown by N-terminal sequencing (starting on Met 1). However, it was not possible to identify the C-terminal end due to conflicting MS results.

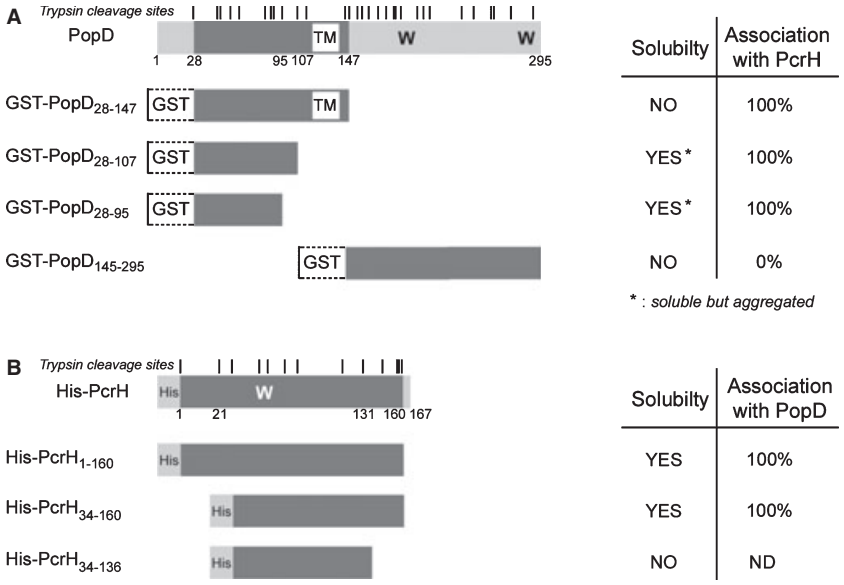

Fig. 2. Delineation of the PopD/PcrH interface. The fragments (dark gray) obtained by limited proteolysis are located on the PopD (A) and PcrH (B) proteins, along with the potential trypsin cleavage sites (short ticks). Tryptophan residues (W) and the predicted transmembrane helix (TM) of PopD are shown. Truncated recombinant proteins were designed and their solubility as well as their capacity to associate with their partner were assessed (tables). ND, not determined.

helices flank the central TPR domain predicted from residues 36 to 137 [11].

In order to map the smallest region of interaction between the two proteins, various constructs encompassing the aforementioned regions of PopD and PcrH were designed and the interaction of the corresponding fragments with the partner protein was assessed. PcrH fragments were produced as N-terminal His-tag fusion proteins. In the case of PopD, $PopD_{28–147}$, $PopD_{28–107}$, $PopD_{28–95}$ and $PopD_{145–295}$ were produced as N-terminal fusions with glutathione *S*-transferase (GST) (Fig. 2A). The presence of the GST tag at the N-terminus was necessary for the expression of the PopD fragments.

To test the interaction between the various PopD fragments and PcrH, PopD- and PcrH-expressing *Escherichia coli* cells were grown separately, then harvested and mixed together before sonication; the soluble fractions were subsequently loaded on a Ni^{2+} column. All three GST-fusion PopD fragments ($PopD_{28–147}$, $PopD_{28–107}$, $PopD_{28–95}$) copurified with His–$PcrH_{1–160}$. After removal of His and GST tags by thrombin cleavage, samples were subjected to native MS [12] and were characterized as stable 1 : 1 complexes (Table 1). However, the C-terminal $PopD_{145–295}$ fragment did not associate with PcrH. Of interest, when purified on their own, the $PopD_{28–147}$ and $PopD_{145–295}$ fragments were insoluble, whereas the $PopD_{28–107}$ and $PopD_{28–95}$ fragments formed large aggregates (Fig. 2A, table). However, PcrH was able to remain soluble and to form 1 : 1 complexes with each of the three N-terminal fragments.

Table 1. Native MS identification of PopD/PcrH complexes.

		Molecular mass (Da)	
Complexes		Experimental	Calculated
$PcrH_{1–160}$	$PopD_{28–147}$	30368 ± 3.7	30365
$PcrH_{1–160}$	$PopD_{28–107}$	26555 ± 1.2	26554
$PcrH_{1–160}$	$PopD_{28–95}$	25191 ± 3.1	25191

In the case of PcrH, three constructs were investigated: $PcrH_{1–160}$ (lacking its last seven amino acids), $PcrH_{34–160}$ (lacking the predicted N-terminal α helix) and $PcrH_{34–136}$ (lacking both N- and C-terminal predicted α helices); they were produced as N-terminal His_6 fusions (Fig. 2B). The two longer fragments were soluble and recognized the same PopD fragment as full-length PcrH (Fig. 2B, table). The third construct was designed to determine whether the TPR domain was sufficient to recognize PopD. As already observed for other TPR-containing proteins, at least one flanking helix was necessary for proper folding and solubility [13].

The hydrophobic residues of PopD are partially accessible to solvent

Intrinsic fluorescence spectra of PcrH, PopD and the PopD/PcrH complex were recorded to evaluate the degree of solvent exposure of tryptophan residues. PopD and PcrH contain two and one tryptophan residues, respectively (Fig. 2). In the case of PopD, the two tryptophan residues (W188 and W288) are localized in the C-terminal region, which is not protected against proteolysis when the protein is complexed with

PcrH (Fig. 2A). The tryptophan of PcrH (W53) is within the TPR domain (Fig. 2B). The fluorescence spectrum of PcrH had a maximum emission intensity (λ_{max}) at 329 nm, which is characteristic of tryptophan residues located in an apolar environment, suggesting that the tryptophan residue of PcrH is buried within the hydrophobic core of the protein (Fig. 3A). By contrast, the fluorescence spectrum of PopD displayed a λ_{max} at 342 nm, revealing tryptophan residues considerably exposed to solvent. The spectrum of the PopD/PcrH complex corresponded to an intermediate situation, with a λ_{max} at 336 nm. This spectrum was similar (with identical λ_{max}) to the sum of the two spectra obtained with the individual proteins. Therefore, the tryptophan residues were, on average, in the same environment in the isolated proteins as in the protein complex, suggesting that W188 and W288 of PopD remained partially exposed to solvent within the 1 : 1 complex. A less probable interpretation of this result would be that, when the proteins are engaged in a complex, one tryptophan residue is within a more polar environment and another residue is within a less polar environment than in the separated proteins.

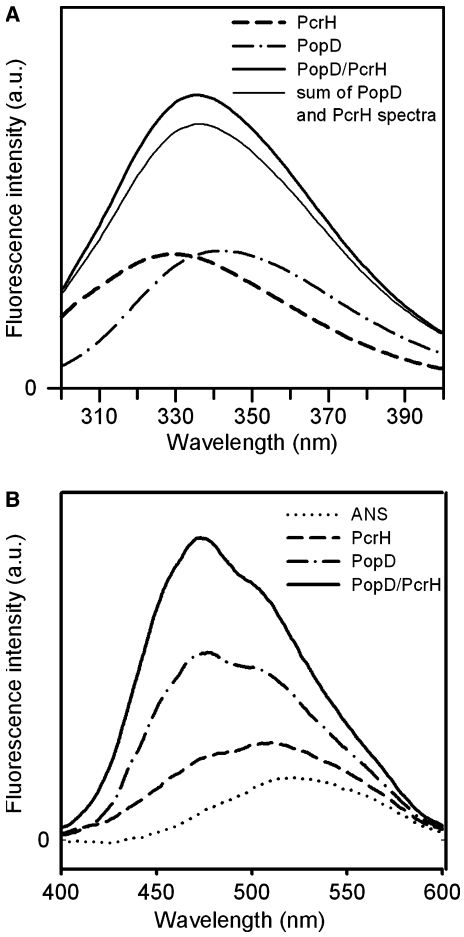

Fig. 3. Hydrophobic residues are buried in a hydrophobic core in PcrH and exposed to solvent in PopD. (A) Fluorescence emission spectra of PcrH (dashed line), PopD (dashed-dotted line) and the PopD/PcrH (solid line) complex were recorded upon excitation at 280 nm. Proteins were diluted to 1 μM in 25 mM Tris/HCl pH 7.2 containing 50 mM NaCl. Spectra are the average of three scans. For comparison, the sum of PcrH and PopD spectra is represented (solid line, thin). (B) ANS fluorescence emission spectra were recorded upon excitation at 370 nm after mixing 10 μM of ANS with 1 μM of PcrH (dashed line), PopD (dashed-dotted line), and the PopD/PcrH complex (solid line). For comparison, a spectrum of ANS in the absence of protein is represented (dotted line).

Intrinsic fluorescence measurements only probe for solvent exposure of tryptophan residues. Therefore, a complementary spectroscopic approach was used to investigate solvent exposure of other hydrophobic residues. Binding of 8-anilinonaphthalene-1-sulfonate (ANS) to organized, structured hydrophobic surfaces accessible to the solvent induces a large increase in fluorescence and a blue-shift on ANS emission spectra. Thus, it is a valuable tool used to characterize partially unfolded proteins [14]. The ANS emission spectrum recorded in the presence of PcrH was close to that obtained with ANS alone, indicating that PcrH was compactly folded with a few ANS-binding sites (Fig. 3B). Conversely, ANS fluorescence increased drastically upon incubation with PopD and the emission maximum shifted from 520 to 470 nm, showing that PopD presents solvent-exposed hydrophobic residues. An increase in ANS fluorescence was also observed when the PopD/PcrH complex was tested. Therefore, it seems likely that PopD presents a considerable number of solvent-exposed hydrophobic residues even when it is bound to PcrH.

PopD has a molten globule conformation

CD measurements were performed in the far UV (from 195 to 250 nm) to evaluate the secondary structure content of the proteins (Fig. 4A). PcrH exhibited a CD spectrum with two minima at 222 and 208 nm, characteristic of a well-folded protein containing mainly α-helical elements. The spectrum of chaperone-free PopD also corresponded to an α-helical secondary structure, but the less marked minimum at 222 nm suggested a slightly smaller amount of α helix. The PopD/PcrH complex was also clearly α-helical and the shape of its spectrum was intermediate between those of PcrH and PopD. Strikingly, the sum of PopD and PcrH spectra nearly superposed with the spectrum of the PopD/PcrH complex, indicating that the secondary structures of PopD and PcrH were conserved in the complex.

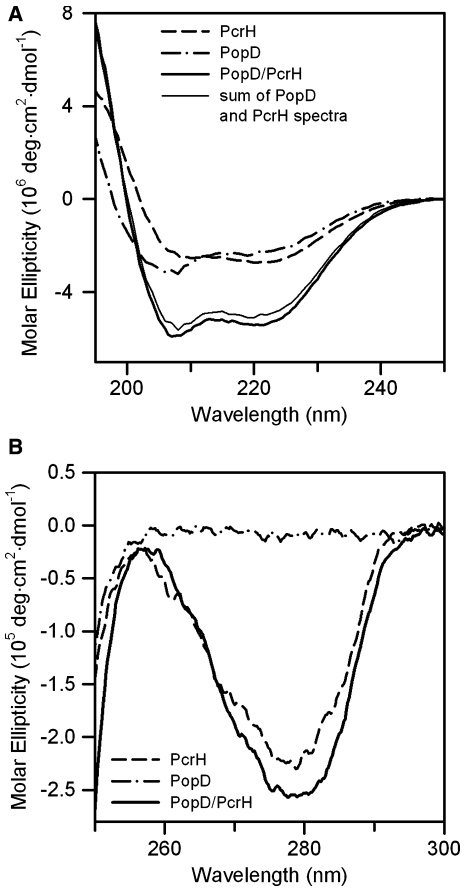

Fig. 4. PopD molten globule conformation revealed by CD spectroscopy. CD spectra of PcrH (dashed line), PopD (dashed-dotted line) and the PopD/PcrH (solid line) complex were recorded in far UV (A) and near UV (B) to assess secondary and tertiary structure, respectively. Protein concentrations were 1 and 10 μM in 25 mM Tris/HCl pH 7.2 containing 50 mM NaCl for far UV and near UV, respectively. Spectra are the average of 10 scans. For comparison, the sum of PcrH and PopD far-UV CD spectra is represented by the thin solid line (A).

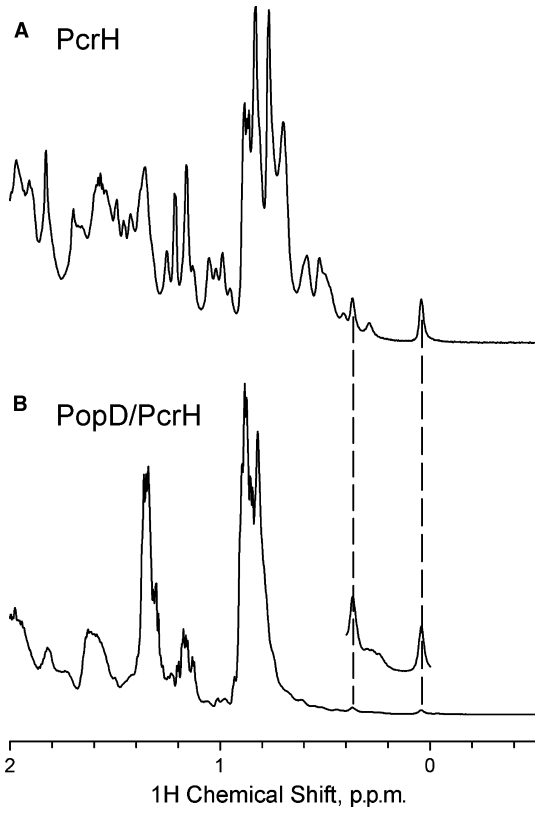

Fig. 5. ^{1}H NMR spectra of PcrH (A) and the PopD/PcrH complex (B). Only the up-field aliphatic region of the spectrum is shown. Spectra were recorded at a protein concentration of 500 μM and a temperature of 37 °C. The ring-current-shifted resonances detected between 1.5 and 0 ppm in the PcrH spectrum are also present in the PopD/PcrH spectrum, despite broad and poorly dispersed resonances in the latter.

CD measurements in the near UV from 250 to 300 nm were used to provide insight into the tertiary fold of the proteins. The minimum at 278 nm observed on the spectrum of PcrH is typical of a protein with a rigid tertiary structure (Fig. 4B). However, the absence of a signal for PopD revealed a lack of stable tertiary structure. Because this protein displays a significant amount of α-helical structure, it could be considered as a molten globule. The near-UV spectrum of the PopD/PcrH complex was very close to the one displayed by PcrH, although the minimum at 278 nm was slightly more pronounced. This indicated that PopD had little or no significant tertiary structure when bound to PcrH and remained in a molten globule conformation in the PopD/PcrH complex.

The 1D NMR spectrum of PcrH was typical of a protein containing a tertiary structure (Fig. 5A), in agreement with the near-UV CD spectra (Fig. 4B). More particularly, ring-current-shifted resonances were detected between 1.5 and 0 p.p.m. These resonances are typical of the stable interactions between side chains within a molecule with tertiary structure. The aspect of the spectrum of the PopD/PcrH complex was very different (Fig. 5B). Beside the peak broadening due to the size of the complex, the spectrum was dominated by broad and poorly dispersed resonances which could be attributed to the presence of PopD. Such a spectrum is consistent with a protein in a molten globule state which undergoes large conformation exchange on a ms time scale [15,16]. However, the ring-current-shifted resonances of PcrH were still detected in the spectrum, although their relative intensities were smaller because PcrH is smaller than PopD (Fig. 2).

PopD adopts a molten globule conformation after *in vitro* refolding

Denaturation/renaturation experiments were performed to assess whether PopD intrinsically folds into a molten globule state. Six molar guanidinium–HCl induced PopD unfolding, as shown by a characteristic far-UV CD spectrum and a λ_{max} at 348 nm (data not shown). Denatured PopD was subsequently diluted into buffer to a lower chaotropic salt concentration, allowing refolding. Far-UV CD spectra showed that PopD recovered its secondary structure content after a 100-fold dilution (Fig. 6A). However, under these conditions, no signal corresponding to tertiary structure was observed in the near-UV CD spectrum. Consistently, the renatured PopD exhibited the same λ_{max} as the untreated PopD. Thus, PopD exhibits the characteristic features of a molten globule after refolding.

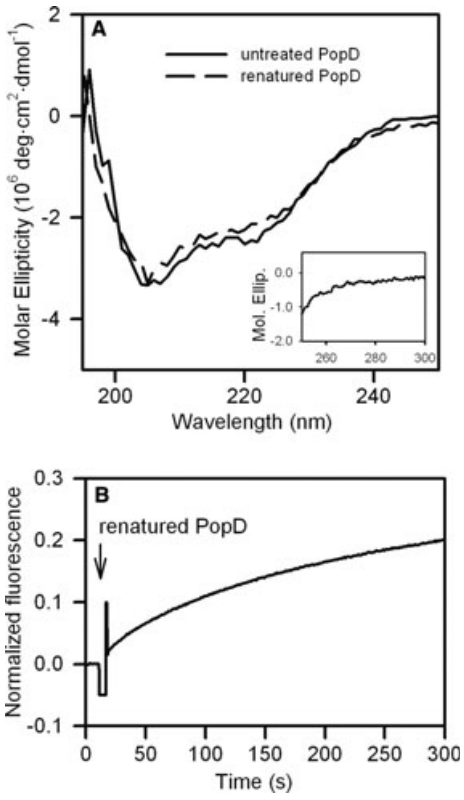

Fig. 6. PopD refolds into a functional molten globule after guanidinium–HCl denaturation. PopD was incubated in 6 M guanidinium to induce complete unfolding. (A) Far-UV CD spectra were recorded after 100-fold dilution (dashed line) and compared with the untreated sample (solid line). After renaturation, PopD does not exhibit near-UV CD signal (insert, the *y*-axis corresponds to molar ellipticity in deg.cm^2.dmol^{-1} × 10^5). (B) Renatured PopD is able to induce liposome permeabilization, detected by the release of sulforhodamine B encapsulated within the lipid vesicles.

Furthermore, the functionality of the renatured PopD was tested by a liposome permeabilization assay. Lipid vesicles were loaded with sulforhodamine B at a concentration leading to its fluorescence self-quenching. Upon membrane leakage, dye release and subsequent dilution in the extra-liposomal buffer induce an increase in fluorescence. PopD was previously shown to induce pore formation [6], and the renatured PopD displays similar properties (Fig. 6B), showing that renaturation leads to the formation of a functional PopD.

Discussion

Type III translocators are thought to mediate the passage of toxic effectors across the membrane of target cells and are associated with chaperones within the bacterial cytoplasm. Unraveling the structural features of these proteins should provide new clues to decipher their mode of action. Here, we show that the PopD translocator of *P. aeruginosa* is bound via its N-terminal region to its chaperone PcrH, and that its structure is partially folded both in the complexed and chaperone-free forms.

Our experiments indicate that PcrH is stably folded independently of PopD binding. Notably, only the N- and C-terminal extremities of the protein could be accessed by trypsin digestion, revealing a stable, protease-resistant TPR core. This domain is responsible for the interaction of the chaperone with the translocators [11,17]. Moreover, the λ_{max} of PcrH's unique tryptophan residue W53, which is located in the first TPR repeat, confirmed that this region is well-folded. In addition, the far-UV CD spectrum of PcrH indicated the presence of mainly α-helical secondary structure, validating the prediction that this class of type III chaperones adopts an all-helical fold [7].

Limited proteolysis, interaction assays and intrinsic fluorescence measurements showed that the N-terminal segment of PopD (from position 28 to 147), encompassing its transmembrane helix, is associated with PcrH. In IpaC, the PopD counterpart in *Shigella* spp., the chaperone-binding domain (CBD) was also mapped to the N-terminal region of the protein [18,19]. In *Yersinia* spp., the N-terminal region of YopD comprising the transmembrane helix, as well as an additional putative C-terminal amphipathic helix, were found to be involved in the interaction with the chaperone, LcrH [20,21]. Two lines of evidence indicate that PopD's C-terminal amphipathic helix is not buried within PcrH: (a) the C-terminal region of PopD is highly sensitive to trypsin, indicating that this region is not sequestered within the PopD/PcrH complex; and (b) the C-terminal tryptophan residues of PopD (W188 and W288) are not buried

in a hydrophobic environment in the complex, as shown by intrinsic fluorescence measurements.

Among the type III chaperones, those which bind effectors have been more extensively studied [1]. Type III effectors are multidomain proteins and the domains responsible for their toxic activity remain natively folded in the complex, while the CBD is wrapped around a chaperone dimer in an extended, nonglobular conformation with elements of secondary structure [22–24]. Similarly to PcrH and PopD, the chaperone SycO was recently shown to mask the membrane localization domain of the effector YopO [25]. Type III chaperones target the effector–chaperone complexes to a hexameric ATPase located at the base of the injectisome, which promotes the dissociation of the secreted proteins from their chaperones as well as their partial unfolding [26]. Indeed, the proteins are secreted through a proteinaceous needle whose internal diameter of ~ 20 Å is too thin to accommodate folded globular proteins [27,28]. It is believed that this unfolding is facilitated by the extended conformation of the effector CBD [23].

Translocators and their cognate chaperones present quite different characteristics. EspB, the PopD homolog in enterohemorrhagic *E. coli*, behaves as a partially folded protein in the absence of its cognate chaperone [29]. Our experiments indicate that PopD is in a molten globule state in both the chaperone-bound and chaperone-free forms, with a high amount of secondary structure (α-helical) but lacking stable tertiary structure. This state has been extensively studied as an intermediate of the protein folding reaction [30]. A protein in a molten globule state is loosely folded and highly flexible, with tryptophan residues and hydrophobic clusters rather exposed to solvent, allowing binding of ANS, a fluorescent probe that recognizes hydrophobic regions. Moreover, PopD's proteolysis susceptibility, the CD measurements and the typical features of the NMR spectrum point to a lack of compact and rigid tertiary structure. Of note, PopD also adopts this molten globule state upon renaturation from the guanidinium-induced unfolded state (Fig. 6). Therefore, the molten globule may correspond to the most stable state of PopD in solution. It is very likely that these observations can be generalized to PopB (E. Faudry and V. Forge, unpublished observations). Like the effectors, translocators must be secreted in order to reach the host cell membrane. Their molten globule conformation further reduces the energetic cost of unfolding prior to secretion.

The molten globule conformation is also beneficial for the interaction of the translocators with membranes because less structural modification is necessary to expose the hydrophobic patches of the protein. α-Pore-forming toxins or toxin-associated translocation domains have been shown to undergo conformation changes toward a molten globule conformation for their insertion into lipid bilayers. In the case of colicin A, staphylococcal α-toxin and diphteria toxin, acidic pH allows proper interaction with the membranes, via a molten globule intermediate [31–34]. This conformation makes the hydrophobic segments available for membrane insertion, while they are buried in the tertiary structure of the soluble state. We previously showed that the chaperone-free PopD, as well as PopB, are able to interact with lipid bilayers and to form pores [6], but the PopD/PcrH complex is not [5]. Thus, although type III secretion translocators adopt a membrane-competent conformation in solution, i.e. molten globule, the chaperone hinders their association with lipid bilayers.

Mutant bacteria lacking the translocator's chaperones grow normally but rapidly degrade the translocators [11,17]. This is certainly related to the molten globule conformation that favors aggregation and misassociation with other proteins. To cope with the threat of incompletely folded or misfolded proteins, bacteria evolved a protein quality control which targets proteins harboring solvent-exposed regions to the degradation machineries [35]. Thus, the molten globule conformation explains the necessity of chaperones to safeguard the translocators and avoid their aggregation [36]. This role is comparable to that of chaperones involved in protein folding, which recognize the molten globule state of proteins and allow isolation of the protein when it is in a state prone to aggregation [37,38].

Experimental procedures

Protein expression and purification

A bicistronic construct containing the *popD* and *pcrH* genes in the pET30b vector was introduced in *E. coli* strain BL21(DE3) allowing the simultaneous expression of both proteins, with PcrH harboring a N-terminal 6-His tag. The 1 : 1 PopD/PcrH complex was purified by Ni^{2+} affinity chromatography and PopD could be subsequently detached from PcrH and purified [5]. PcrH was expressed from the pET15b/*pcrH* plasmid [5] and purified to homogeneity using a standard Ni^{2+} affinity chromatography.

Proteolysis

In preliminary experiments, the action of eight different proteases on the PopD/PcrH complex was assessed by SDS/PAGE. The best results were obtained with trypsin at a protease/complex ratio of 1 : 1000 and incubation on ice, in 20 mM Tris/HCl, 0.1 M NaCl pH 8.0. After 3 h, the

sample was loaded onto a Superdex 200 column equilibrated in 20 mM Tris/HCl, 0.1 M NaCl pH 8.0 and protein peaks were analyzed by SDS/PAGE. Peptides were identified by MS and N-terminal sequencing.

Expression of truncated PcrH and PopD

DNA fragments encoding $PcrH_{1-160}$, $PcrH_{34-160}$ and $PcrH_{34-136}$ were produced by PCR and subsequently cloned in the pET-Duet1 vector. DNA fragments encoding the truncated $PopD_{28-147}$ and $PopD_{145-295}$ were produced by PCR, whereas $PopD_{28-107}$ and $PopD_{28-95}$ fragments were obtained by the introduction of a stop codon using site-directed mutagenesis on the $PopD_{28-147}$ template (QuikChange™ Site-directed Mutageneis Kit, Stratagene, La Jolla, CA). PopD constructs were subsequently cloned in a pGEX4T vector. All clones were verified by DNA sequencing. The proteins were produced in *E. coli* BL21(DE3) and JM109 cells for His–PcrH and GST–PopD fusion proteins, respectively. To test complex formation, the different BL21(DE3) and JM109 cells were mixed during sonication in the presence of 1% Chaps. The different supernatants obtained after centrifugation for 45 min at 39 000 ***g*** were purified on Hitrap-Chelating column (GE Healthcare, London, UK) with a linear imidazole gradient. Copurification of GST-PopD proteins with His–PcrH was assessed by SDS/PAGE. The purified complexes were digested by thrombin at room temperature for one hour and the two tags (GST and His6) were removed by combining glutathione and Ni^{2+} columns.

MS analysis

Identification of fragments generated by digestion was performed by using a PE Sciex (Toronto, Ontario, Canada) API IIII+ triple quadrupole mass spectrometer equipped with an ionspray source. Samples were loaded on C4 protein Macrotrap cartridge (Michrom, Auburn, CA) desalted with H_2O 0.1% trifluoroacetic acid. Proteins were eluted with 60% of CH_3CN/H_2O 9/1 (v/v) 0.1% trifluoroacetic acid. The spectra were recorded in the 500–1500 range of mass-to-charge (*m/z*) ratios.

The three PopD/PcrH complexes with concentrations of ~ 30 μM were dialyzed in 25 mM ammonium bicarbonate pH 7.9 and analyzed by native MS. The measurements were performed by using a Q-TOF Micro mass spectrometer (Waters, Manchester, UK) equipped with an electrospray ion source. The mass spectra were recorded in the 2000–6100 *m/z* range; spectra were acquired and data were processed with MASSLYNX 4.0 (Waters).

Intrinsic fluorescence

Tryptophan fluorescence emission spectra were measured on a Jasco FP-6500 fluorimeter with an excitation wavelength set at 280 nm (10 nm slit) and emission monitored at 100 $nm \cdot min^{-1}$ from 300 to 400 nm (5 nm slit) with three accumulations. Proteins were diluted to 1 μM in a buffer containing 25 mM Tris/HCl pH 7.2, 50 mM NaCl and were tested in a 1 cm optical path cell. Buffer spectra were subtracted from sample spectra using Jasco SPECTRA ANALYSIS software. The sum of the PcrH and PopD spectra could be compared with the spectrum of the PopD/PcrH complex because the three experimental spectra were obtained at the same protein concentration of 1 μM and in the same conditions.

ANS fluorescence

ANS emission spectra were measured on a Jasco FP-6500 fluorimeter with the excitation wavelength set at 370 nm (5 nm slit) and emission monitored at 100 $nm \cdot min^{-1}$ from 400 to 600 nm (5 nm slit). Three accumulations were recorded and buffer spectra were subtracted. ANS was solubilized in water and the concentration was determined by measuring the optical density at 350 nm and considering a molar extinction coefficient of 4950 $cm^{-1} \cdot M^{-1}$ [39]. Proteins were diluted to 1 μM in a buffer containing 25 mM Tris/HCl pH 7.2, 50 mM NaCl and were tested in a 1 cm optical path cell with ANS concentrations varying from 1 to 10 μM.

CD

Far-UV and near-UV CD spectra were acquired on a Jasco J-810 spectrophotometer with a scan speed of 50 $nm \cdot min^{-1}$ at 20 °C. Spectra are the average of 10 scans with the baseline corrected with buffer spectra. For far-UV CD spectra, 0.1 cm path length cells were used with a protein concentration of 1 μM and the signal was recorded from 250 to 195 nm. Near-UV CD spectra were obtained from 320 to 250 nm, using 1 cm cells and a protein concentration of 10 μM. Buffers are the same as for fluorescence measurements. CD measurements were normalized to protein concentration and presented as molar ellipticity.

NMR spectroscopy

One-dimensional ^1H spectra were recorded with a 800 MHz spectrometer (Varian, Palo Alto, CA). The protein concentration was 500 μM in $NaCl/P_i$ at pH 7.3 and the temperature was kept at 37 °C during acquisition of spectra.

Guanidininium–HCl denaturation and renaturation

PopD was unfolded in 6 M guanidinium–HCl by dissolving solid guanidinium–HCl in the samples at room temperature. Samples were diluted 100-fold in 25 mM Tris/HCl

pH 7.2 containing 50 mM NaCl and CD spectra were recorded as described above. Near-UV CD spectra were obtained with a 20 cm optical path cell. Lipid vesicle permeabilization assays were performed as described previously [6] with vesicles made of phosphatidylcholine/phosphatidylserine (8 : 2, mol/mol). Fluorescence intensity was normalized to the maximum of fluorescence signal obtained after addition of Triton X-100 to the samples.

Acknowledgements

We thank Grégory Vernier and Sylvie Elsen for helpful discussions, David Lemaire for mass spectrometry measurements, Jean-Pierre Andrieu for N-terminal sequencing and Adrien Favier for help with NMR (NMR facilities; IBS; Grenoble). This study was supported in part by the French cystic fibrosis association 'Vaincre la Mucoviscidose' and the CEA-DSV program 'Membrane proteins'.

References

1 Cornelis GR (2006) The type III secretion injectisome. *Nat Rev Microbiol* **4**, 811–825.
2 Buttner D & Bonas U (2002) Port of entry – the type III secretion translocon. *Trends Microbiol* **10**, 186–192.
3 Coombes BK & Finlay BB (2005) Insertion of the bacterial type III translocon: not your average needle stick. *Trends Microbiol* **13**, 92–95.
4 Goure J, Pastor A, Faudry E, Chabert J, Dessen A & Attree I (2004) The V antigen of *Pseudomonas aeruginosa* is required for assembly of the functional PopB/PopD translocation pore in host cell membranes. *Infect Immun* **72**, 4741–4750.
5 Schoehn G, Di Guilmi AM, Lemaire D, Attree I, Weissenhorn W & Dessen A (2003) Oligomerization of type III secretion proteins PopB and PopD precedes pore formation in *Pseudomonas*. *EMBO J* **22**, 4957–4967.
6 Faudry E, Vernier G, Neumann E, Forge V & Attree I (2006) Synergistic pore formation by type III toxin translocators of *Pseudomonas aeruginosa*. *Biochemistry* **45**, 8117–8123.
7 Pallen MJ, Francis MS & Futterer K (2003) Tetratricopeptide-like repeats in type-III-secretion chaperones and regulators. *FEMS Microbiol Lett* **223**, 53–60.
8 Menard R, Sansonetti P, Parsot C & Vasselon T (1994) Extracellular association and cytoplasmic partitioning of the IpaB and IpaC invasins of *S. flexneri*. *Cell* **79**, 515–525.
9 Neyt C & Cornelis GR (1999) Role of SycD, the chaperone of the *Yersinia* Yop translocators YopB and YopD. *Mol Microbiol* **31**, 143–156.
10 Holmstrom A, Olsson J, Cherepanov P, Maier E, Nordfelth R, Pettersson J, Benz R, Wolf-Watz H & Forsberg A (2001) LcrV is a channel size-determining component of the Yop effector translocon of *Yersinia*. *Mol Microbiol* **39**, 620–632.
11 Broms JE, Edqvist PJ, Forsberg A & Francis MS (2006) Tetratricopeptide repeats are essential for PcrH chaperone function in *Pseudomonas aeruginosa* type III secretion. *FEMS Microbiol Lett* **256**, 57–66.
12 Heck AJ & Van Den Heuvel RH (2004) Investigation of intact protein complexes by mass spectrometry. *Mass Spectrom Rev* **23**, 368–389.
13 Main ER, Xiong Y, Cocco MJ, D'Andrea L & Regan L (2003) Design of stable alpha-helical arrays from an idealized TPR motif. *Structure* **11**, 497–508.
14 Semisotnov GV, Rodionova NA, Razgulyaev OI, Uversky VN, Gripas AF & Gilmanshin RI (1991) Study of the 'molten globule' intermediate state in protein folding by a hydrophobic fluorescent probe. *Biopolymers* **31**, 119–128.
15 Balbach J, Forge V, van Nuland NA, Winder SL, Hore PJ & Dobson CM (1995) Following protein folding in real time using NMR spectroscopy. *Nat Struct Biol* **2**, 865–870.
16 Balbach J, Forge V, Lau WS, Jones JA, van Nuland NA & Dobson CM (1997) Detection of residue contacts in a protein folding intermediate. *Proc Natl Acad Sci USA* **94**, 7182–7185.
17 Edqvist PJ, Broms JE, Betts HJ, Forsberg A, Pallen MJ & Francis MS (2006) Tetratricopeptide repeats in the type III secretion chaperone, LcrH: their role in substrate binding and secretion. *Mol Microbiol* **59**, 31–44.
18 Page AL, Fromont-Racine M, Sansonetti P, Legrain P & Parsot C (2001) Characterization of the interaction partners of secreted proteins and chaperones of *Shigella flexneri*. *Mol Microbiol* **42**, 1133–1145.
19 Harrington AT, Hearn PD, Picking WL, Barker JR, Wessel A & Picking WD (2003) Structural characterization of the N terminus of IpaC from *Shigella flexneri*. *Infect Immun* **71**, 1255–1264.
20 Francis MS, Aili M, Wiklund ML & Wolf-Watz H (2000) A study of the YopD–lcrH interaction from *Yersinia pseudotuberculosis* reveals a role for hydrophobic residues within the amphipathic domain of YopD. *Mol Microbiol* **38**, 85–102.
21 Tengel T, Sethson I & Francis MS (2002) Conformational analysis by CD and NMR spectroscopy of a peptide encompassing the amphipathic domain of YopD from *Yersinia*. *Eur J Biochem* **269**, 3659–3668.
22 Luo Y, Bertero MG, Frey EA, Pfuetzner RA, Wenk MR, Creagh L, Marcus SL, Lim D, Sicheri F, Kay C *et al.* (2001) Structural and biochemical characterization of the type III secretion chaperones CesT and SigE. *Nat Struct Biol* **8**, 1031–1036.
23 Stebbins CE & Galan JE (2003) Priming virulence factors for delivery into the host. *Nat Rev Mol Cell Biol* **4**, 738–743.

24 Lilic M, Vujanac M & Stebbins CE (2006) A common structural motif in the binding of virulence factors to bacterial secretion chaperones. *Mol Cell* **21**, 653–664.
25 Letzelter M, Sorg I, Mota LJ, Meyer S, Stalder J, Feldman M, Kuhn M, Callebaut I & Cornelis GR (2006) The discovery of SycO highlights a new function for type III secretion effector chaperones. *EMBO J* **25**, 3223–3233.
26 Akeda Y & Galan JE (2005) Chaperone release and unfolding of substrates in type III secretion. *Nature* **437**, 911–915.
27 Cordes FS, Komoriya K, Larquet E, Yang S, Egelman EH, Blocker A & Lea SM (2003) Helical structure of the needle of the type III secretion system of *Shigella flexneri*. *J Biol Chem* **278**, 17103–17107.
28 Deane JE, Roversi P, Cordes FS, Johnson S, Kenjale R, Daniell S, Booy F, Picking WD, Picking WL, Blocker AJ *et al*. (2006) Molecular model of a type III secretion system needle: implications for host-cell sensing. *Proc Natl Acad Sci USA* **103**, 12529–12533.
29 Hamada D, Kato T, Ikegami T, Suzuki KN, Hayashi M, Murooka Y, Honda T & Yanagihara I (2005) EspB from enterohaemorrhagic *Escherichia coli* is a natively partially folded protein. *FEBS J* **272**, 756–768.
30 Arai M & Kuwajima K (2000) Role of the molten globule state in protein folding. *Adv Protein Chem* **53**, 209–282.
31 van der Goot FG, Gonzalez-Manas JM, Lakey JH & Pattus F (1991) A 'molten-globule' membrane-insertion intermediate of the pore-forming domain of colicin A. *Nature* **354**, 408–410.
32 Muga A, Gonzalez-Manas JM, Lakey JH, Pattus F & Surewicz WK (1993) pH-dependent stability and membrane interaction of the pore-forming domain of colicin A. *J Biol Chem* **268**, 1553–1557.
33 Vecsey-Semjen B, Mollby R & van der Goot FG (1996) Partial C-terminal unfolding is required for channel formation by staphylococcal alpha-toxin. *J Biol Chem* **271**, 8655–8660.
34 Chenal A, Savarin P, Nizard P, Guillain F, Gillet D & Forge V (2002) Membrane protein insertion regulated by bringing electrostatic and hydrophobic interactions into play. A case study with the translocation domain of diphtheria toxin. *J Biol Chem* **277**, 43425–43432.
35 Wickner S, Maurizi MR & Gottesman S (1999) Post-translational quality control: folding, refolding, and degrading proteins. *Science* **286**, 1888–1893.
36 Feldman MF & Cornelis GR (2003) The multitalented type III chaperones: all you can do with 15 kDa. *FEMS Microbiol Lett* **219**, 151–158.
37 Walter S & Buchner J (2002) Molecular chaperones – cellular machines for protein folding. *Angew Chem Int Ed Engl* **41**, 1098–1113.
38 Hartl FU & Hayer-Hartl M (2002) Molecular chaperones in the cytosol: from nascent chain to folded protein. *Science* **295**, 1852–1858.
39 Weber G & Young LB (1964) Fragmentation of bovine serum albumin by pepsin. I. the Origin of the acid expansion of the albumin molecule. *J Biol Chem* **239**, 1415–1423.